Korean J. Chem. Eng., 38(1), 55-63 (2021)
DOI: 10.1007/s11814-020-0685-0

pISSN: 0256-1115
eISSN: 1975-7220

Effects of sludge pyrolysis temperature and atmosphere on characteristics of biochar and gaseous products

Shuai Guo, Xiaoyan Xiong, Deyong Che, Hongpeng Liu, and Baizhong Sun†

School of Energy and Power Engineering, Northeast Electric Power University, Jilin 132012, China
(*Received 11 June 2020 • Revised 9 September 2020 • Accepted 21 September 2020*)

Abstract−In view of the importance of inert-atmosphere sludge pyrolysis for effective waste recycling and carbon emission reduction, this study probed the effects of temperature (300-700 °C) and atmosphere (100% N_2, 10 CO_2/90% N_2, or 100% CO_2) on the properties of biochar and gases obtained by sludge pyrolysis in a horizontal tube furnace. The emissions of NO, SO_2, H_2S, and CO increased with increasing temperature, as the inhibitory effect of CO_2 on the formation of these gases (observed at <500 °C) concomitantly weakened and was superseded by the reaction of CO_2 with carbon at higher temperature to afford gaseous products. The specific surface area (S_{BET}) and pore volume of the biochar produced in the presence of CO_2 increased with increasing temperature up to 500 °C, while at higher temperatures the inhibitory effect of CO_2 on pore structure development resulted in a decreased S_{BET} and an increased macropore content. These results show that pyrolysis is an effective treatment method for sludge; it can remove 48% N and 50% S in sludge and mitigate the emission of polluting gases. When CO_2 participates in the pyrolysis reaction, the S_{BET} of biochar increases significantly. In general, sludge biochar has the potential to be applied as fuel and as an adsorbent.

Keywords: Sewage Sludge, Pyrolysis, CO_2 Atmosphere, Biochar, Pore Structure

INTRODUCTION

Municipal sludge, which is unavoidably produced during sewage treatment, is a heterogeneous mixture of water, proteins, lipids, carbohydrates, nucleic acids, phenols, ash, pathogens, heavy metals, polychlorinated biphenyls, dioxins, and other harmful substances [1]. The rapid urbanization of China has significantly increased the amount of municipal sludge produced, which, when not promptly dealt with, can cause severe environmental and health problems upon discharge into the environment [2]. Currently, the increasingly stringent sludge management regulations limit the application of direct sludge discharge, and thus necessitate the further development of alternative disposal methods, such as landfilling, composting, and incineration [3]. Landfilling and composting are the main methods of sludge disposal in China, accounting for 60-65% and 10-15% of the total disposed sludge, respectively [4]. However, such common disposal techniques may cause secondary pollution of the groundwater and soil, which renders the thermochemical treatment of sludge (e.g., pyrolysis, gasification, or incineration) a viable alternative [5]. Among these methods, sludge pyrolysis is advantageous in that it is low-cost and exhibits the ability to simultaneously afford solid, liquid, and gaseous products [6,7]. In addition, organic pollutants and pathogenic microorganisms are removed and the volume of waste is significantly reduced. Another advantage of sludge pyrolysis is the production of biochar. This porous solid product can be used for agricultural soil remediation, the absorption of heavy metal contaminants [8,9], and other applications.

Previous studies into sludge pyrolysis have deepened our understanding of the processes involved, and have more recently, focused on the effects of the pyrolysis conditions [10-12]. More specifically, although the thermal decomposition of sludge has mostly been carried out in inert gases such as N_2, some studies probed the effects of a CO_2 atmosphere on sludge pyrolysis, as this approach allows one to recycle torrefaction-produced CO_2, and thereby promote the generation of carbon-negative power, while also reducing CO_2 emissions [13-15]. Since the participation of CO_2 is known to affect the pyrolysis behavior of coal and biomass, Tan et al. [16] studied the nutrient characteristics of straw biochar, and found that the N, P, and K content of biochar pyrolyzed in a CO_2 atmosphere was higher than that in N_2 atmosphere. In addition, Zhu et al. [17] studied the pyrolysis of bio-oil distillation residues in different atmospheres and found that below 600 °C the biochar yield and calorific value were higher in a CO_2 atmosphere than in a N_2 atmosphere. Guizani et al. [18] found that the CO content of the pyrolysis gas increased upon the introduction of CO_2 due to the homogeneous and heterogeneous reactions of the latter with gases, tars, and char. Moreover, CO_2 introduction is known to affect the pH, conductivity, and elemental composition of biochar produced by sludge pyrolysis [19]. Combined thermogravimetric-Fourier transform infrared (TG-FTIR) spectroscopic analysis of coal pyrolysis showed that the substitution of N_2 with CO_2 enhanced the volatile release efficiency and prevented calcite decomposition [14]. Guizani et al. [18] studied rapid biomass pyrolysis, revealing that CO_2 influenced the amount and composition of the gaseous products as well as the carbon yield and performance. The reaction between CO_2 and nascent char above 600 °C was shown to proceed at a considerably high rate because of the concomitant occurrence of thermal crack-

†To whom correspondence should be addressed.
E-mail: sunbaizhong@126.com

ing, thereby resulting in additional mass loss [19]. The pyrolysis atmosphere was therefore concluded to affect the yield, composition, and calorific value of the solid, liquid, and gaseous pyrolysis products.

The pyrolysis atmosphere also affects the development of the biochar pore structure. In this context, Tan et al. [16] found that the pore structure development during straw pyrolysis was strongly affected by the choice of atmosphere (CO_2 or N_2), with CO_2 favoring the development of the desired micro-, meso-, and macroporous structures, in addition to the production of biochar with a high specific surface area. In another report, biochar obtained in a CO_2 atmosphere demonstrated a higher porosity (19-47%) than that obtained in N_2 [19]. Depending on the feedstock type, the use of CO_2 during pyrolysis can enhance the cleavage of benzene rings in addition to the hydroxyl, methyl, and methylene groups present in biochar, as well as weaken the interactions between H and the biochar matrix [16-20]. These reactions result in increased quantities of $H^{\bullet}$ radicals, which can combine with other free radicals to favor the formation of volatiles [21]. The above reactions afford biochar with a specific surface area and pore volume higher than those of biochar produced under N_2. Thus, the use of CO_2 instead of N_2 changes the pyrolysis behavior of the biomass and increases the environmental remediation efficacy of the produced biochar, thereby offering additional possibilities for the management of anthropogenic CO_2 [22]. Although biomass pyrolysis in CO_2 has been extensively investigated, only a few studies have dealt with the effects of CO_2 on the pyrolytic production of biochar and gas from sludge; hence, these effects deserve further attention. Furthermore, the pore structure of biochar produced under different pyrolysis atmospheres has rarely been discussed. To close this knowledge gap, the present work probes the effect of the atmosphere (100% N_2, 10% CO_2/90% N_2, and 100% CO_2) and temperature (300-700 °C) on the characteristics of biochar and gases (SO_2, H_2S, CO, and NO) produced by municipal sludge pyrolysis in a tubular horizontal furnace. Notably, this study mainly focuses on sludge biochar, with no specific studies conducted on the tar produced during sludge pyrolysis.

MATERIALS AND METHODS

1. Materials

Municipal sludge, obtained from a wastewater treatment plant in Jilin City, Jilin Province, China, was dried in a drying chamber at 105 °C for 24 h, ground to a 100-150 mesh size, and stored in a sealed tube until required for pyrolysis. Table 1 lists the main properties of the sludge, indicating its high contents of ash and volatiles. The volatile compounds were the main source of heat release during sludge combustion and the main ash components (70 wt% in total) were identified as SiO_2, Al_2O_3, and Fe_2O_3.

2. Pyrolysis System

The pyrolysis system comprised a gas supply section, a reaction section (with an approximately 100 mm-long thermostatic reaction zone), and a collecting and testing section (Fig. 1). The dried and ground sludge was heated at 300-700 °C in 100% N_2, 10% CO_2/90% N_2, or 100% CO_2. In each run, the dried sludge sample (1±0.01 g) was loaded into a crucible and placed in the furnace,

Table 1. Main characteristics of the sludge

Sample	Ultimate analysis (wt%, db*)				Proximate analysis (wt%, db)			Higher heating value (kJ/kg)	
	C	H	N	S	Volatiles	Fixed carbon	Ash		
Sludge	19.68	3.33	2.99	0.62	32.88	5.78	61.34	8,200	
	SiO_2	Al_2O_3	Fe_2O_3	P_2O_5	CaO	MgO	K_2O	SO_3	Na_2O
Ash (wt%)	41.90	18.10	10.40	7.03	4.76	2.53	2.40	1.58	1.21

*db=dry basis.

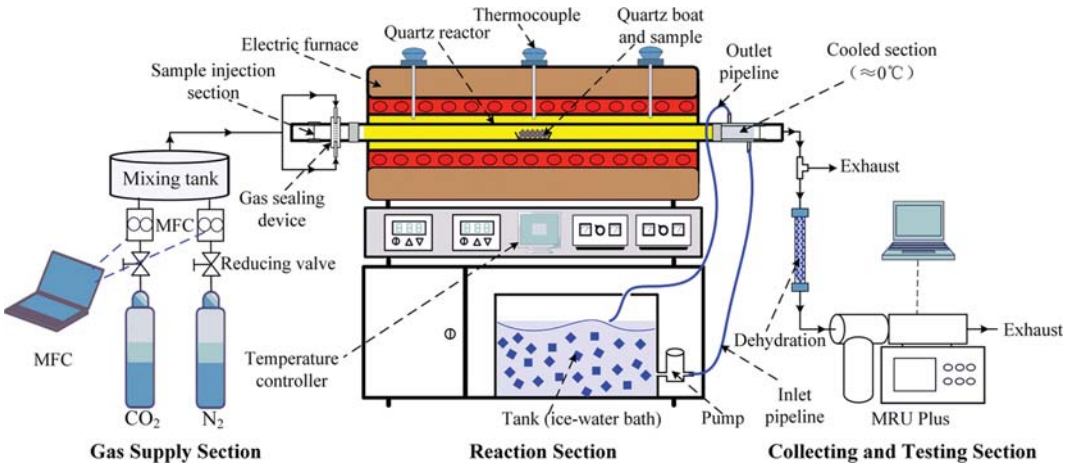

Fig. 1. Diagram of the experimental pyrolysis system used.

Table 2. Elemental compositions, HHVs, and yields of the biochar samples produced under different conditions (BC-*x*-*y*, where *x* and *y* denote the pyrolysis temperature (°C) and CO_2 content (%), respectively)

Sample	Biochar yield (%)	C_{db}%	H_{db}%	N_{db}%	S_{db}%	HHV (kJ/kg)
BC-300-0	77.35±0.42	15.14	1.69	2.06	0.34	5,820.32
BC-400-0	70.15±0.68	11.47	1.03	1.54	0.36	4,000.87
BC-500-0	68.13±0.45	10.35	0.71	1.27	0.35	3,825.43
BC-600-0	66.13±0.34	9.99	0.46	1.10	0.36	3,260.46
BC-700-0	64.59±0.40	9.33	0.26	0.82	0.37	3,152.72
BC-300-10	78.12±0.21	15.32	1.74	2.12	0.38	5,029.91
BC-400-10	71.05±0.65	11.96	1.15	1.63	0.36	4,502.85
BC-500-10	69.2±0.40	10.91	0.76	1.33	0.33	3,525.47
BC-600-10	66.91±0.09	10.29	0.44	1.12	0.33	3,371.07
BC-700-10	64.96±0.27	8.16	0.20	0.72	0.34	2,019.82
BC-300-100	78.45±0.16	15.65	1.74	2.21	0.39	6,395.69
BC-400-100	70.99±0.70	12.41	1.19	1.66	0.36	3,892.80
BC-500-100	69.35±0.58	11.08	0.71	1.33	0.30	3,824.00
BC-600-100	67.48±0.44	9.98	0.42	1.10	0.27	2,469.48
BC-700-100	62.57±0.29	5.97	0.17	0.66	0.25	1,064.19

which had been purged with N_2 (99.99%) at a flow rate of 1 L/min for 15 min prior to heating to create an oxygen-free atmosphere. A mass flow controller (MFC) was used to control the N_2/CO_2 flow. The furnace was heated to the desired temperature at a rate of 10 °C/min; this temperature was maintained for 1 h. The NO, H_2S, SO_2, and CO produced during pyrolysis were detected using a flue gas analyzer (VARIO luxx, MRU GmbH, Germany). When pyrolysis was complete, the obtained biochar was cooled to ambient temperature and weighed to determine the biochar yield (Table 2) from the biochar weight (W_2) and the dry weight of the sewage sludge subjected to pyrolysis (W_1) ($100\% \times W_2/W_1$). All experiments were carried out in triplicate to ensure reproducibility and consistency.

3. Characterization of the Pyrolysis Products

3-1. Biochar Elemental Analysis and Calorific Value Determination

The N, H, and C content of the produced biochar was determined using an automatic elemental analyzer (EA3000, EuroVector S.P.A., Italy) with combustion at 950 °C. The S content was determined using an infrared sulfur determination instrument (SDS350, Hunan Sundy Science and Technology Co., Ltd., China). Bomb calorimetry (SDAC6000 calorimeter, Hunan Sundy Science and Technology Co., Ltd., China) was used to determine the higher heating value (HHV) of the biochar according to ASTM E-711 [23].

3-2. Analysis of the Biochar Pore Structure

Based on the Brunauer-Emmett-Teller (BET) multilayer adsorption theory, the isothermal adsorption of N_2 at 77 K was studied using an automatic adsorption device (TriStar II, USA). Prior to the adsorption measurements, the sample was degassed under vacuum for 1 h at 150 °C. The BET specific surface area (S_{BET}), average pore size (D), and total pore volume (V) were then determined by application of the BET equation, the Barrett-Joyner-Halenda (BJH) model, and single-point adsorption total pore volume analysis, respectively. The size distributions of the micro-, meso-, and macropores were analyzed based on experimental data and using density functional theory calculations.

RESULTS AND DISCUSSION

1. Influence of Temperature and Atmosphere on the Gaseous Pyrolysis Products

Relatively high nitrogen and sulfur content within the sludge (Table 1) can result in the formation of large amount of NO_x and SO_x during pyrolysis. These gaseous pollutants are responsible for acid rain, photochemical smog, enhancement of the greenhouse effect, and the increased depletion of stratospheric ozone. In addition, CO released during pyrolysis will cause carbon loss within the biochar. Based on this, the release behavior of the various gaseous pyrolysis products was examined herein.

As shown in Figs. 2 and 3, the formation of gaseous pyrolysis products was affected by the pyrolysis temperature and the atmosphere. In N_2, the emissions of NO, H_2S, SO_2, and CO increased with increasing temperature (Fig. 2) due to the concomitant increase in the degree of sludge pyrolysis and the decomposition of volatiles. The NO and CO emissions were highest at 700 °C (Fig. 2(a) and 2(d)), while those of SO_2 and H_2S were highest at 600 °C (Fig. 2(b) and 2(c)). In sludge, nitrogen mainly exists in the form of ammonia, protein, pyrrolidine, and pyridine. Upon increasing the temperature, the ammonia and ammonium salts present in the sludge decompose to afford nitrogen-containing gases [24]. In N_2, the CO emission only slightly increased upon increasing the temperature to 600 °C, although a drastic change was observed at higher temperature (Fig. 2(a)). CO is obtained by the decomposition of carbonyl and hydroxyl groups at low temperature or by the fracture of oxygen-containing heterocyclic rings and ether bonds at high temperature [25]. Furthermore, the emissions of SO_2 and H_2S, the main sulfur-containing gases produced by sludge pyrolysis, increased with increasing temperature, prior to slightly decreasing again at 700 °C. Thus, high temperature promoted the formation of CO, which, in turn, favored the decomposition of sulfur-containing species in the sludge, decreased the S content of the biochar, increased the emission of sulfur-containing gases such as H_2S

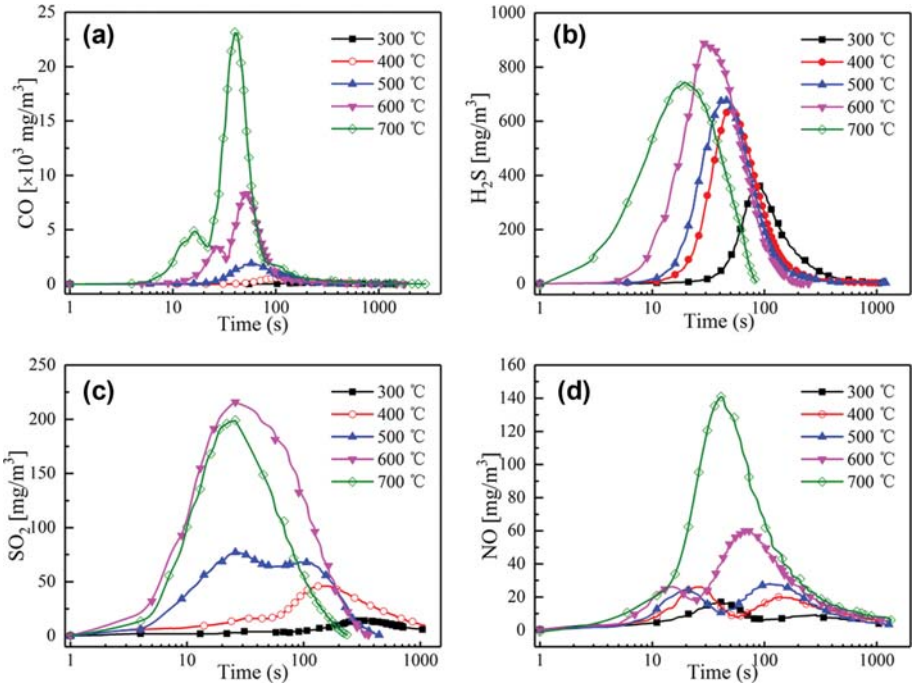

Fig. 2. Release profiles of (a) CO, (b) H_2S, (c) SO_2, and (d) NO during sludge pyrolysis at different temperatures in 100% N_2.

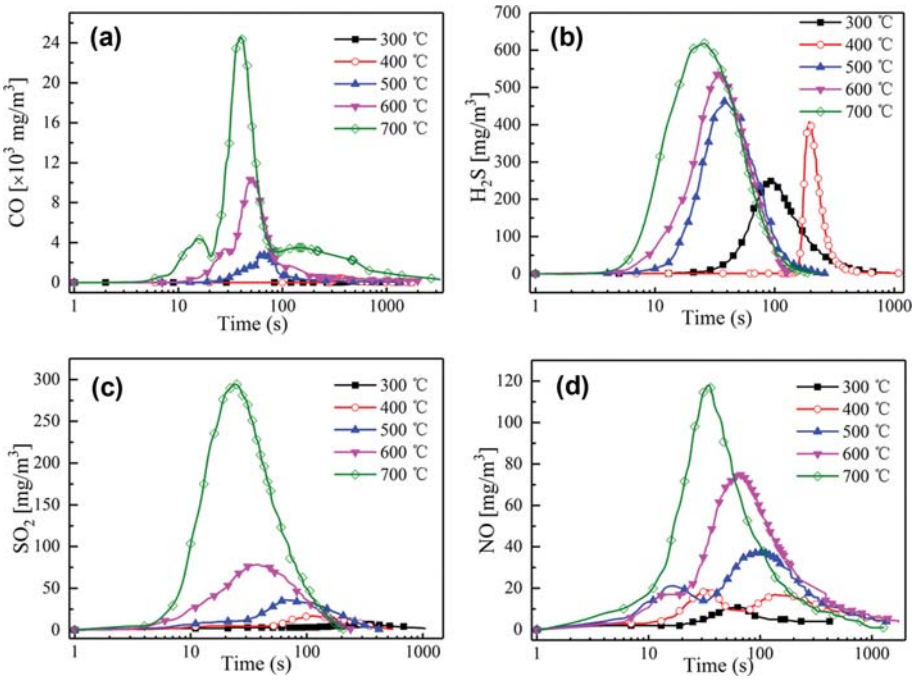

Fig. 3. Release profiles of (a) CO, (b) H_2S, (c) SO_2, and (d) NO during sludge pyrolysis at different temperatures in 100% CO_2.

and COS, and favored the conversion of SO_2 to COS (R1-R2) [26]. In addition, upon increasing the temperature, the alkali/alkaline earth metal sulfates (MSO_4) present in the sludge were able to react with CO to form SO_2 (R3) [27].

$$CO+SO_2 \rightarrow S+CO_2 \quad (R1)$$

$$CO+S \rightarrow COS \quad (R2)$$

$$MSO_4+CO \rightarrow MO+CO_2+SO_2 \quad (R3)$$

Notably, the emissions of NO, SO_2, and H_2S obtained in CO_2 (Fig. 3) were lower than those obtained in N_2. At low temperature (300-400 °C), H_2S was released later than at high temperature, and in smaller amounts than in N_2 (Fig. 3(b)). These findings indicate that CO_2 had a mild effect on the decomposition of stable sulfur

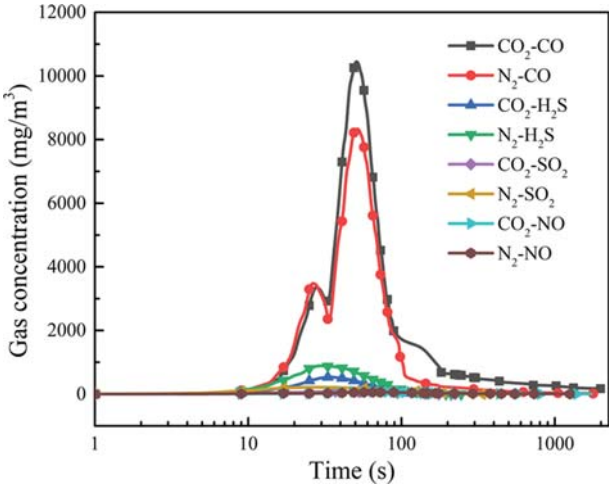

Fig. 4. Release profiles of CO, H_2S, SO_2, and NO during sludge pyrolysis at 600 °C in different atmospheres.

compounds at low temperature, while promoting the formation of H_2S and SO_2 above 600 °C (Fig. 3(b) and 2(c)). At high temperature, CO_2 aided C-S bond cleavage, promoting the decomposition of sulfur-containing compounds and the formation of sulfur-based free radicals, which reacted with internal hydrogen/oxygen and external CO_2 [28]. Moreover, above 600 °C, CO_2 reacted with carbon to form CO, and the extent of this reaction became more pronounced with an increase in temperature [29]. This is consistent with the results reported by Kim et al., who believe that the use of CO_2 promotes the pyrolysis of volatile substances formed in pyrolysis and increases the production of CO at temperature above 550 °C [30]. Therefore, the emission of CO in the CO_2 atmosphere exceeded that in the N_2 atmosphere. As shown in Fig. 3, the gasification reaction between C and CO_2 was not clear below 700 °C.

Furthermore, at the same pyrolysis temperature (600 °C), gas production in the two different pyrolysis atmospheres showed variations, as presented in Fig. 4. More specifically, the release of SO_2 and H_2S in the CO_2 atmosphere was lower than in the N_2 atmosphere, indicating that the CO_2 atmosphere can inhibit the release of sulfur-containing gases and thereby reduce the emission of pollutants. It was also found that the reaction atmosphere has little impact on NO emission. However, in a CO_2 atmosphere, CO emission is higher than that in an N_2 atmosphere, which is caused by the Boudouard reaction between carbon and CO_2.

2. Effects of the Temperature and Atmosphere on the Biochar Properties

2-1. Effects of the Pyrolysis Temperature and Atmosphere on the Biochar Yield

Table 2 lists the biochar yield obtained at different temperatures and in different atmospheres, showing that upon increasing the temperature (i.e., from 300 to 700 °C), the yield of biochar produced under N_2 decreased from 77.35 to 64.59%, with the largest decrease being observed at 300-400 °C. This trend is similar to the results of Wang et al. [12], who reported that the percentage of biochar yield from sludge declined steadily from 68.65 to 58.11% with an increase in the pyrolysis temperature from 300 to 700 °C. This was owing to the substantial decomposition of organic substances in the sludge during pyrolysis. Therefore, this temperature range is believed to represent the onset of volatile production from the sludge. The reduction in yield upon increasing the temperature was triggered by the degradation of organic matter, dehydration due to hydroxyl group removal, the loss of chemically bound moisture, and, at higher temperature, the production of aromatic structures accompanied by the loss of large amount of CO_2, CO, H_2O, and H_2 [32].

It was also found that in a 10% CO_2/90% N_2 atmosphere, the biochar yield decreased from 78.12 to 64.96%, while in 100% CO_2, it decreased from 78.45 to 62.57% at 300-700 °C. Compared with N_2, CO_2 positively affected biochar production between 300 and 600 °C by inhibiting the volatilization or cracking of oxygenated functional groups in the sludge to produce oxygen-containing gases such as CO_2 and CO [32]. Furthermore, the abovementioned positive influence can be ascribed to the fact that CO_2 has a larger molar weight than N_2, and hence, contact between the sludge particles and CO_2 is less efficient, according to the diffusion theory [33,34]. Moreover, in 100% CO_2, the carbon yield sharply decreased at a temperature >600 °C, likely due to the Boudouard reaction, in which CO_2 reacts with sludge carbon to produce CO [35].

Thus, the effects of the pyrolysis atmosphere on biochar production were concluded to be temperature-dependent; below 600 °C the production of biochar is favored in CO_2, although this promotional effect weakens with increasing temperature. Moreover, the efficiency of biochar production decreased with increasing CO_2 content.

2-2. Influence of the Temperature and Atmosphere on the Calorific Value of Biochar

As shown in Table 1 and Table 2, under different reaction conditions, the HHV range of biochar is 1,064.19-6,395.69 kJ/kg, and its calorific value is lower than that of raw sludge. This is caused by the increased ash content and decreased carbon content after sludge pyrolysis. It is well known that a high HHV is related to a lower ash content and higher carbon content [36]. As shown in Table 2, upon increasing the temperature, the HHV of biochar decreased; this change is significant in the range of 300-400 °C due to the large concomitant compositional change. In addition, the change in carbon content, which affects the biochar HHV, was most pronounced in the same temperature range, and the CO_2 content was also found to affect the HHV, i.e., an increase in the HHV upon increasing the CO_2 content between 300 and 500 °C. Moreover, the biochar produced below 600 °C in CO_2 presented a higher HHV than that produced in N_2 at the same temperature, which was ascribed to the different effects of these gases on sludge cracking and volatilization [32]. These results are consistent with those reported by Zhu et al., who believe that CO_2 will inhibit the decomposition of carbon-containing structures at 600 °C and will retain a higher carbon content than in a N_2 atmosphere [17]. However, the reverse was observed at 700 °C, possibly because at this temperature CO_2 reacts with carbon to reduce the carbon content of the biochar and thereby decrease its calorific value [31].

2-3. Effects of the Pyrolysis Temperature and Atmosphere on the Biochar Composition

As shown in Table 2, the C, H, N, and S content of the biochar produced in N_2 decreased with increasing temperature due to the

Table 3. Pore structure parameters of the biochar samples produced under different conditions (BC-*x*-*y*, where *x* and *y* denote the pyrolysis temperature (°C) and CO_2 content (%), respectively)

Sample	S_{BET} (m^2/g)	V_{ads} (cm^3/g)	V_{des} (cm^3/g)	D_{ads} (nm)	D_{des} (nm)
BC-300-0	30.41	0.08	0.09	10.79	8.64
BC-300-10	29.13	0.08	0.09	11.03	8.76
BC-300-100	30.35	0.09	0.09	11.18	8.79
BC-400-0	57.70	0.11	0.12	9.43	7.86
BC-400-10	59.31	0.12	0.13	10.10	8.35
BC-400-100	61.41	0.13	0.13	8.54	8.30
BC-500-0	58.34	0.13	0.13	10.22	9.06
BC-500-10	59.33	0.13	0.13	10.18	9.03
BC-500-100	59.99	0.12	0.12	9.50	8.47
BC-600-0	51.83	0.12	0.13	10.77	9.51
BC-600-10	51.01	0.12	0.13	10.65	9.41
BC-600-100	50.86	0.12	0.13	11.20	9.88
BC-700-0	43.59	0.11	0.12	11.73	10.35
BC-700-10	39.68	0.11	0.11	12.30	10.76
BC-700-100	33.47	0.10	0.10	12.94	11.28

concomitant loss of volatiles, and, hence, surface functional group elements [37,38]. Note that since sludge has higher content of protein and some heterocyclic compounds than other biomasses, it is richer in N and S [39,40]. A pyrolysis treatment can remove 48% N and 50% S in sludge. In addition, the low S and N content of biochar suggest that its combustion as a fuel would have a low impact on the environment. Furthermore, the decomposition of sludge protein (at 360-525 °C) decreases the N content in biochar, while dehydration, decarboxylation, and demethanation reactions contribute to C and H removal during pyrolysis [41].

It was also found that the carbon content of the biochar produced in N_2 at 300-500 °C was lower than that of the biochar produced in CO_2 due to the inhibitory effect of the latter gas on the volatilization and decomposition of carbon-containing structures [31]. At temperature >500 °C, the carbon content of the biochar significantly decreased with increasing CO_2 content, while the N, H, and S content remained relatively constant. Thus, CO_2 appeared to behave as an inert gas below 500 °C, while influencing the biochar properties at higher temperatures through the Boudouard reaction and the reaction between the sludge carbon and sludge minerals (R4-R5) [42]. Udayanga et al. [43] showed that at 660 °C, $CaCO_3$ decomposition occurred during pyrolysis (R6) and the Boudouard reaction (R4) was induced in the presence of CO_2.

$$C+CO_2 \rightarrow 2CO \quad (R4)$$

$$CaSO_4+2C \rightarrow CaS+2CO_2 \quad (R5)$$

$$CaCO_3 \rightarrow CaO+CO_2 \quad (R6)$$

These results therefore indicated that the pyrolysis temperature influenced the elemental composition of the biochar to a larger extent than the pyrolysis atmosphere. More specifically, the C, H, N, and S content of the biochar decreased with increasing temperature, whereby the largest change was observed within the range of 300-400 °C. At any given temperature, CO_2 had the greatest impact on the carbon content, behaving as an inert gas and inhibiting the decomposition of carbon-containing structures below 600 °C, while engaging in reactions to promote carbon volatilization at higher temperature.

3. Influence of the Temperature and Atmosphere on the Biochar Pore Structure

Table 3 lists the pore structure parameters of the biochar samples produced under different conditions, revealing that in N_2, the S_{BET} increased from 30.41 to 58.34 m^3/g upon an increase in temperature from 300 to 500 °C, while the pore volume increased from 0.08 to 0.12 cm^3/g. Above 500 °C, the S_{BET} and pore volume decreased, i.e., pore structure development was promoted by low-temperature (i.e., <500 °C) pyrolysis. This effect was ascribed to the increased removal of volatile organic matter within this temperature range, which resulted in pore unblocking [44]. The decrease in S_{BET} and pore volume above 500 °C was attributed to the increased proportion of sludge ash observed at high temperature, which hindered pore formation [10]. As shown in Table 1, the sludge ash was rich in SiO_2, Al_2O_3, Fe_2O_3, and P_2O_5, and the high content of alkaline metals (Na, K), alkaline earth metals (Ca, Mg), and Si, Cl, S, P, and Fe in the sludge could result in the formation of low-melting-temperature silicates, which are able to fill and block existing pores [45]. Furthermore, the S_{BET} of the sludge biochar (30.41-58.34 m^3/g) was smaller than that of biochar produced from agricultural and forestry wastes, such as straw and livestock manure (121.2-222.5 m^3/g); this was ascribed to the high cellulose content of these wastes and the resulting facile micropore formation upon heating [46].

Fig. 5(a) presents the N_2 adsorption/desorption isotherms of the biochar produced at different temperatures in N_2. According to the IUPAC classification [47], these isotherms are of type IV and feature type H2 hysteresis loop behavior, which indicates that (i) the corresponding biochar mainly contains mesopores (pore width= 2-50 nm) [48], (ii) capillary condensation could occur in the pores, and (iii) the pores exhibit narrow necks and wide bodies, i.e., they could be denoted as "ink-bottle pores." Upon increasing the rela-

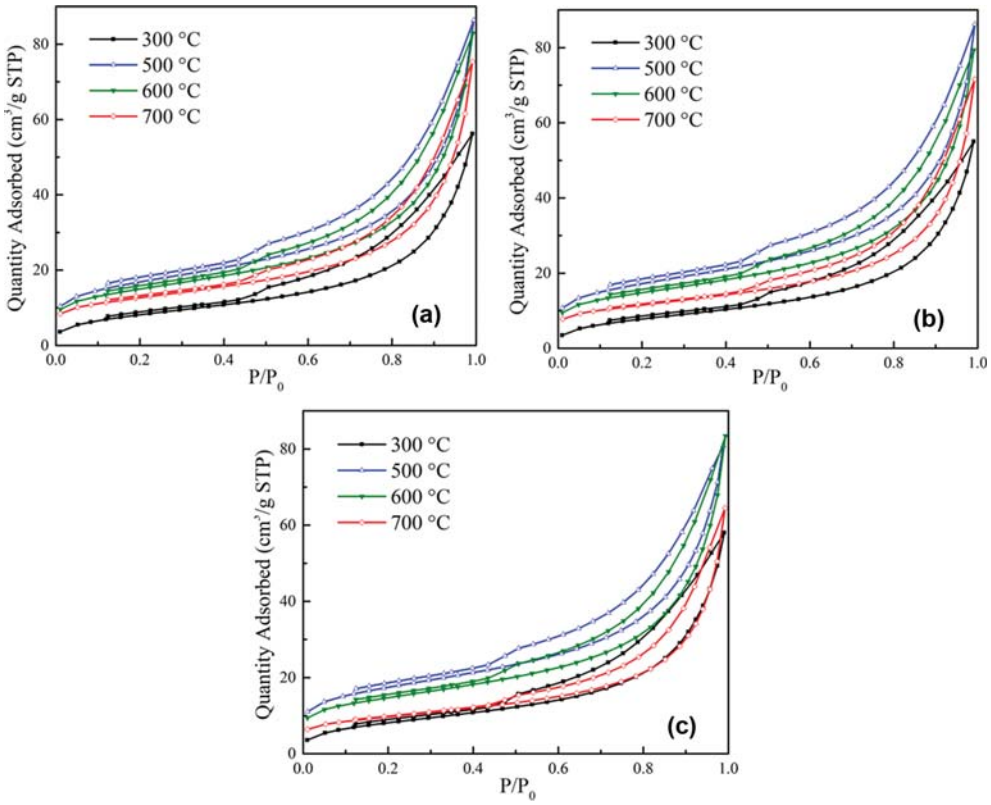

Fig. 5. N_2 adsorption/desorption isotherms of the biochar samples produced at different temperatures in (a) 100% N_2, (b) 10% CO_2/90% N_2, and (c) 100% CO_2.

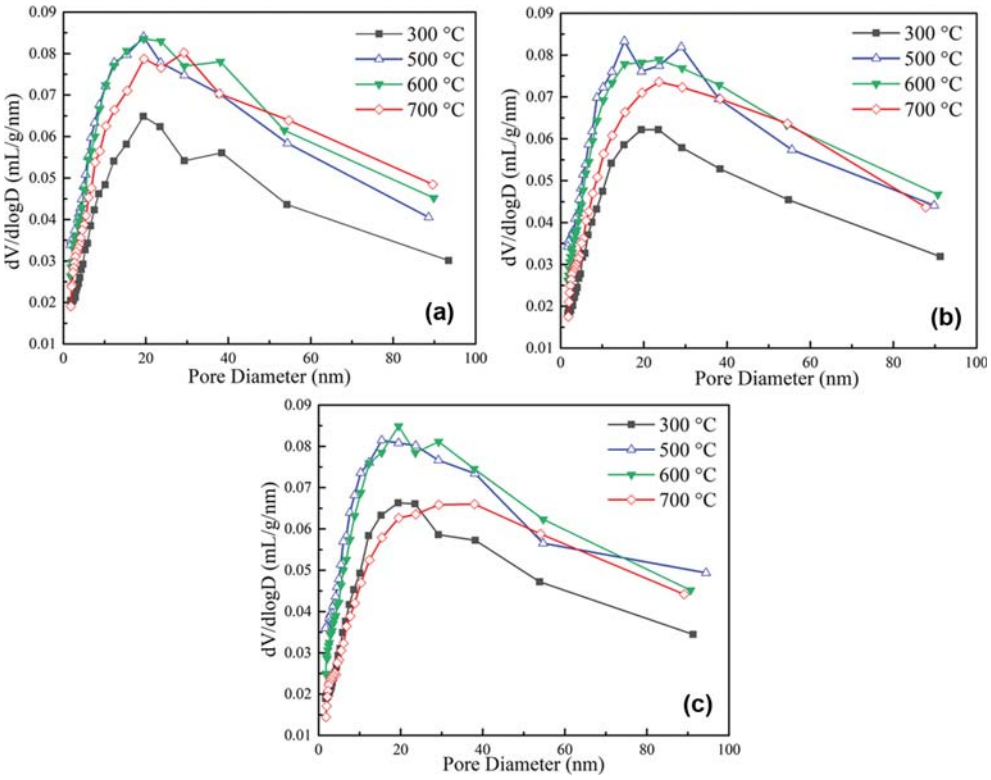

Fig. 6. Pore size distributions of the biochar samples produced at different temperatures in (a) 100% N_2, (b) 10% CO_2/90% N_2, and (c) 100% CO_2.

Table 4. Comparison among some characteristics of the obtained biochar samples and threshold values of the EBC, IBI and Italian fertilization decree standards

Parameter	Biochar	EBC	IBI	Italian decree
Carbon content [% w/w] db	5.97-15.65	Not required	Class 1: ≥60 Class 2: ≥30 & <60 Class 3: ≥10 & <30	Not required
H/C	0.29-1.36	≤0.7	≤0.7	≤0.7
Surface area [m^2/g]	29.13-59.99	Declaration; better >150	Declaration	Declaration

tive pressure (P/P_0), the adsorption amount of each sample significantly increased in the medium-pressure region ($0.2<P/P_0<0.8$), which indicated the presence of mesopores (2 nm<D<50 nm) in the biochar. In the high-pressure region ($P/P_0>0.8$), the degree of adsorption also rapidly increased with increasing P/P_0 up to $P/P_0\approx1$, but did not reach saturation, thereby indicating that the biochar contained a certain number of large pores (D>50 nm). The corresponding pore size distribution (Fig. 6(a)) gave an average pore size range of 2-90 nm, which further confirms the presence of meso- and macropores within the biochar. Furthermore, the number of mesopores gradually increased with an increase in temperature from 300 to 600 °C, while a further temperature increase decreased the number of mesopores by inducing their collapse, resulting in the formation of macropores.

Interestingly, the use of CO_2 instead of N_2 significantly contributed to the increase in the S_{BET}. More specifically, the S_{BET} and pore volume of the biochar produced in CO_2 at 300-500 °C were higher than those of the biochar produced in N_2 and increased with an increase in CO_2 content. However, at high temperature (>500 °C), CO_2 inhibited development of the biochar pore structure. In addition, the N_2 adsorption/desorption isotherms of biochar produced in CO_2 (Figs. 5(b) and 2(c)) were identical to those of the samples produced in N_2: they were type IV isotherms and featured type H2 hysteresis. Notably, the adsorption capacity increased upon increasing the temperature and the CO_2 content. The pore size of biochar produced in CO_2 at 300-500 °C was within 2-90 nm, thereby mostly corresponding to mesopores. Upon increasing the temperature and the CO_2 content, the number of mesopores decreased, while the number of macropores increased owing to pore expansion caused by the gasification reaction between CO_2 and carbon at high temperature [45,49].

Finally, the S_{BET} of the biochar produced in CO_2 at 300-500 °C exceeded that of the biochar produced in N_2 at the same temperature, i.e., a biochar sample with a superior adsorption performance was obtained in CO_2. Between 300 and 500 °C, an increase in the CO_2 content also induced an increase in the S_{BET}, while above 500 °C, CO_2 inhibited pore structure development.

4. Comparison with Different Biochar Criteria

A comparison among some properties of the biochar samples and the threshold values of three biochar standards - the European Biochar Certificate (EBC), the International Biochar Initiative (IBI), and the Italian decree for soil fertilizers (D.L. 29 APRILE 2010, N. 75) - was conducted to determine whether the obtained biochar samples in this work would conform to these limitations [50].

As shown in Table 4, only IBI defines the carbon content range of biochar. As the carbon content of sludge biochar is between 5.97 and 15.65%, it belongs to IBI class 3. The H/C molar ratio, which is one of the most important features of biochar, represents the degree of carbonization as well as the stability of biochar. Table 4 shows that part of the sludge biochar meets the H/C molar ratio requirements. Specifically, within the range of 600-700 °C, the H/C molar ratio of the biochar produced in this study conforms to the standards and the ratio remains relatively constant under different atmospheres. Therefore, the H/C molar ratio of sludge biochar is mainly influenced by the pyrolysis temperature. Finally, the S_{BET} of biochar greatly affects its application as an adsorbent or fuel. The EBC requirements state that it should preferably be higher than 150 m^2/g; however, the S_{BET} of the sludge biochar samples produced in this study are all lower than 60 m^2/g due to the high ash content within the sludge biochar. Therefore, the pore structure characteristics, especially the specific surface area, should be improved through various methods in future work.

CONCLUSIONS

Herein, an examination into the effects of temperature and atmosphere on sludge pyrolysis in a horizontal tube furnace is reported. It was found that the CO, SO_2, H_2S, and NO emissions increased with increasing pyrolysis temperature, with CO as the main gaseous product. In the temperature range of 300-600 °C, the CO emission obtained for pyrolysis in a CO_2 atmosphere was lower than that under N_2 atmosphere, sharply increasing at temperatures >600 °C in the former case. In addition, the increased production of SO_2 and H_2S in a CO_2 atmosphere indicated that CO_2 promotes the decomposition of sulfur-containing compounds to afford biochar with a relatively low S content. Furthermore, upon increasing the temperature, the C, H, N, and S content of the biochar decreased; additionally, the CO_2 atmosphere had a greater impact on the carbon content. At low temperature (<600 °C), CO_2 behaved as an inert gas, inhibiting carbon structure decomposition, whereas at higher temperature (>600 °C), CO_2 behaved as a reactive gas, promoting carbon volatilization. Analysis of the resulting biochar pore structure showed that the S_{BET} and pore volume increased with increasing temperature between 300 and 500 °C, with the values obtained for CO_2 exceeding those obtained for N_2. Above 500 °C, the facile collapse of the biochar mesopores in CO_2 led to macropore formation. Overall, the obtained results indicate that the pyrolysis of sludge not only reduces the quantity of harmful substances

generated by the direct treatment of sludge, but also produces biochar with low nitrogen and sulfur content. Moreover, the introduction of CO_2 in the pyrolysis process can improve the pore structure of biochar and provide a foundation for the use of biochar in energy storage or as an adsorbent in the future.

ACKNOWLEDGEMENTS

This work was supported by National Natural Science Funds for Young Scholars of China (51806033); National Key Technologies Research and Development Program (2018YFB0905104); Jilin Provincial Science and Technology Development Program (20190201096JC).

REFERENCES

1. Y. Tian, J. Zhang, W. Zuo, L. Chen, Y. N. Cui and T. Tan, *Environ. Sci. Technol.*, **47**, 3498 (2013).
2. S. Zandi, B. Nemati, D. Jahanianfard, M. Davarazar, Y. Sheikhnejad, A. Mostafaie, M. Kamali and T. M. Aminabhavi, *J. Environ. Manage.*, **247**, 462 (2019).
3. G. Yang, G. G. Zhang and H. C. Wang, *Water Res.*, **78**, 60 (2015).
4. S. J. Sun, Z. B. Zhao, B. Li, L. X. Ma, D. L. Fu, X. Z. Sun, S. Thape, J. M. Shen, H. Qi and Y. N. Wu, *Environ. Pollut.*, **245**, 764 (2019).
5. Y. H. Feng, T. C. Yu, D. Z. Chen, G. L. Xu, L. Wan, Q. Zhang and Y. Y. Hu, *Energy Fuels*, **32**, 581 (2018).
6. I. A. Aldobouni, A. B. Fadhil and I. K. Saied, *Energy Sources, Part A: Recov., Utilization, Environ. Effects*, **37**, 2617 (2015).
7. A. B. Fadhil, M. A. Alhayali and L. I. Saeed, *Fuel*, **210**, 165 (2017).
8. L. Y. Gao, J. H. Deng, G. F. Hang, K. Li, K. Z. Cai, Y. Liu and F. Huang, *Bioresour. Technol.*, **272**, 114 (2019).
9. Y. Yue, L. Cui, Q. M. Lin, G. T. Li and X. R. Zhao, *Chemosphere*, **173**, 551 (2017).
10. H. R. Yuan, T. Lu, H. Y. Huang, D. D. Zhao, N. Kobayashi and Y. Chen, *J. Anal. Appl. Pyrolysis*, **112**, 284 (2015).
11. W. D. C. Udayanga, A. Veksha, A. Giannis and T. T. Lim, *Waste Manag.*, **83**, 131 (2019).
12. X. D. Wang, Q. Q. Chi, X. J. Liu and Y. Wang, *Chemosphere*, **216**, 698 (2019).
13. Y. He and X. Q. Ma, *Bioresour. Technol.*, **189**, 71 (2015).
14. L. B. Duan, C. S. Zhao, W. Zhou, C. R. Qu and X. P. Chen, *Energy Fuels*, **23**, 3826 (2009).
15. B. Prabowo, M. Aziz, K. Umeki, H. Susanto, M. Yan and K. Yoshikawa, *Appl. Energy*, **158**, 97 (2015).
16. Z. G. Tan, J. H. Zou, L. M. Zhang and Q. Y. Huang, *J. Mater. Cycles. Waste Manag.*, **20**, 1036 (2018).
17. X. F. Zhu, K. Li, L. Q. Zhang, X. Wu and X. F. Zhu, *Energy Convers. Manag.*, **157**, 288 (2018).
18. C. Guizani, J. E. Sanz and S. Salvador, *Fuel*, **116**, 310 (2014).
19. M. Kończak, P. Oleszczuk and K. Różyło, *J. CO_2 Util.*, **29**, 20 (2019).
20. Y. H. Bai, P. Wang, L. J. Yan, C. L. Liu, F. Li and K. Xie, *J. Anal. Appl. Pyrolysis*, **104**, 202 (2013).
21. S. P. Gao, J. T. Zhao, Z. Q. Wang, J. F. Wang, Y. T. Fang and J. J. Huang, *J. Fuel Chem. Technol.*, **41**, 257 (2013).
22. Z. W. Liu, F. X. Zhang, H. L. Liu, F. Ba, S. J. Yan and J. H. Hu, *Bioresour. Technol.*, **249**, 983 (2018).
23. International A. ASTM E711-87. Standard test method for gross calorific value of refuse-derived fuel by the bomb calorimeter (2004).
24. Z. X. Xu, L. Xu, J. H. Cheng, Z. X. He, Q. Wang and X. Hu, *Fuel Process. Technol.*, **182**, 37 (2018).
25. R. Xiong, L. Dong, J. Yu, X. F. Zhang, L. Jin and G. W. Xu, *Fuel Process. Technol.*, **91**, 810 (2010).
26. A. Attar, *Fuel*, **57**, 201 (1978).
27. Y. Q. Duan, L. B. Duan, E. J. Anthony and C. S. Zhao, *Fuel*, **189**, 98 (2017).
28. H. Q. Guo, X. L. Wang, F. R. Liu, M. J. Wang, H. Zhang, R. S. Hu and Y. F. Hu, *Fuel*, **206**, 716 (2017).
29. H. Q. Wang, K. K. Li, Z. H. Guo, M. X. Fang, Z. Y. Luo and K. F. Cen, *Carbon Resour. Convers.*, **1**, 94 (2018).
30. J. H. Kim, J. I. Oh, J. Lee and E. E. Kwon, *Energy*, **179**, 163 (2019).
31. Z. Khanmohammadi, M. Afyuni and M. R. Mosaddeghi, *Waste Manag. Res.*, **33**, 275 (2015).
32. D. W. Cho, G. Kwon, K. Yoon, Y. F. Tsang, Y. S. Ok and E. E. Kwon, *Energy Convers. Manag.*, **145**, 1 (2017).
33. Y. H. Song, Q. N. Ma and W. J. He, *Energy Fuels*, **31**, 217 (2017).
34. L. Wang, J. Sandquist, G. Varhegyi and B. M. Güell, *Energy Fuels*, **27**, 6098 (2013).
35. R. Wen, B. Yuan, Y. Wang, W. M. Cao, Y. Liu, Y. Jia and Q. Liu, *Environ. Sci. Pollut. Res.*, **25**, 5105 (2018).
36. Y. Liu, C. M. Ran, A. A. Siyal, Y. M. Song, Z. H. Jiang, J. J. Dai, P. Chtaeva, J. Fu, W. Y. Ao, Z. Y. Deng and T. H. Zhang, *J. Hazard. Mater.*, **396**, 122619 (2020).
37. X. Y. He, Z. X. Liu, W. J. Niu, L. Yang, T. Zhou, D. Qin, Z. Y. Niu and Q. X. Yuan, *Energy*, **143**, 746 (2018).
38. T. Chen, Y. X. Zhang, H. T. Wang, W. J. Lu, Z. Y. Zhou, Y. C. Zhang and L. L. Ren, *Bioresour. Technol.*, **164**, 47 (2014).
39. P. Sannigrahi, A. J. Ragauskas and G. A. Tuskan, *Biofuel. Bioprod. Biorefin.*, **4**, 209 (2010).
40. M. E. Sánchez, J. A. Menéndez, A. Domínguez, J. J. Pis, O. Martínez and L. F. Calvo, *Biomass Bioenergy*, **33**, 933 (2009).
41. Z. G. Liu and G. H. Han, *Fuel*, **158**, 159 (2015).
42. Z. H. Wang, X. Q. Ma, Z. L. Yao, Q. H. Yu, Z. Wang and Y. S. Lin, *Appl. Therm. Eng.*, **128**, 662 (2018).
43. W. D. C. Udayanga, A. Veksha, A. Giannis, G. Lisak and T. T. Lim, *Energy Convers. Manag.*, **196**, 1410 (2019).
44. A. Zielińska, P. Oleszczuk, B. Charmas, J. S. Zięba and S. P. Patkowska, *J. Anal. Appl. Pyrolysis*, **112**, 201 (2015).
45. J. Pallarés, A. G. Cencerrado and I. Arauzo, *Biomass Bioenergy*, **115**, 64 (2018).
46. J. H. Windeatt, A. B. Ross, P. T. Williams, P. M. Forster, M. A. Nahil and S. Singh, *J. Environ. Manage.*, **146**, 189 (2014).
47. K. S. W. Sing, D. H. Everett, R. A. W. Haul, L. Moscou, R. A. Pierotti and J. Rouquerol, *Pure. Appl. Chem.*, **57**, 603 (1985).
48. A. Downie, A. Crosky and P. Munroe, *Physical properties of biochar, in: Biochar for environmental management: science and technology*, Earthscan, London (2009).
49. C. Jindarom, V. Meeyoo, B. Kitiyanan, T. Rirksomboon and P. Rangsunvigit, *J. Chem. Eng.*, **133**, 239 (2007).
50. E. Miliotti, D. Casini, L. Rosi, G. Lotti, A. M. Rizzo and D. Chiaramonti, *Biomass Bioenergy*, **139**, 105593 (2020).